Four-coloring model on the square lattice: A critical ground state

Jané Kondev and Christopher L. Henley
Laboratory of Atomic and Solid State Physics, Cornell University, Ithaca, New York 14853
(Received 6 April 1995)

We study critical properties of the four-coloring model, which is given by the equal-weighted ensemble of all possible edge colorings of the square lattice with four different colors. We map the four-coloring model onto an interface model for which we propose an effective Gaussian field theory, which allows us to calculate correlation functions of operators in the coloring model. The critical exponents are given by the stiffness of the interface, which we calculate *exactly* using recent results on the statistical topography of rough interfaces. Our numerical exponents, from Monte Carlo simulations of the four-coloring model, are in excellent agreement with the analytical calculations. These results support the conjecture that the scaling limit of the four-coloring model is given by the $SU(4)_{k=1}$ Wess-Zumino-Witten model. Moreover, we show that our effective field theory *is* the free-field representation of the $SU(4)_{k=1}$ Wess-Zumino-Witten model. Finally, we discuss connections to loop models, and some predictions of finite temperature properties of a particular Potts model for which the four-coloring model is the ground state.

I. INTRODUCTION

Over the years the ground-state ensembles of certain two-dimensional classical spin models have been found to exhibit critical behavior. The first such ground-state ensemble was encountered in the antiferromagnetic Ising model on the triangular lattice.[1,2] The correlation functions of operators constructed from the Ising spins in the ground-state ensemble were found to decay with distance as power laws with various exponents.

Other known models with critical ground states are the six-vertex model[3] and the closely related three-state antiferromagnetic Potts model on the square lattice,[4] the three-state antiferromagnetic Potts model on the Kagomé lattice,[5,6] and the $O(n)$ model on the honeycomb lattice.[7,8] Other models that are of this type are the antiferromagnetic Ising model of general spin on the triangular lattice,[9,10] the noncrossing dimer model, and the dimer-loop model,[11] both defined on the square lattice.

It has recently been shown that the ground-state properties of all the known classical spin models with critical ground states can be analyzed by mapping the original spin model onto an interface model.[12] This analysis is equivalent (by a duality) to the Coulomb gas method, which has been used successfully for calculating exact critical exponents of many two-dimensional lattice models.[13]

In this paper we study the properties of the ground state of a very particular variant of the four-state antiferromagnetic Potts model on the square lattice. This model was first introduced by Read[14] as a generalization of the three-state antiferromagnetic Potts model on the Kagomé lattice. The Potts spins live on the *bonds* of the square lattice. At each vertex, the Potts spins living on the bonds that meet at that particular vertex interact pairwise antiferromagnetically with equal strength.

Our study of the ground-state properties of the Potts model was inspired by two questions: First, whether the ground-state ensemble is indeed critical, and if so, what are the scaling dimensions of the different operators? Second, are the critical correlations in the ground state correctly described by the SU(4) Wess-Zumino-Witten (WZW) model[15] at level $k = 1$, as conjectured by Read?[14] The $SU(4)_{k=1}$ WZW model is a conformal field theory (CFT) with conformal charge $c = 3$, and a known spectrum of scaling dimensions of the primary fields.[16]

An interesting question that has been raised recently is how, and whether, the introduction of frustration (or in this case constraints) can lead to large values of the conformal charge ($c > 1$) in two dimensional lattice models. Large values of c have been observed in the fully frustrated XY model on the square lattice,[17] and more recently in the fully packed loop model on the honeycomb lattice.[7] Just as in the fully packed loop model, the value of the conformal charge that is found in the four-coloring model can be understood by mapping this model to an interface model. The basic idea is that the constraints in these two models require that the heights of the interface have more than one component. This interface can be therefore thought of as an embedding of the two-dimensional lattice in a higher dimensional target-space. If the interface is rough, the field theory which describes the long-wavelength fluctuations of the interface will have a conformal charge given by the dimensionality of the target space, as is well known from the theory of the bosonic string.[18] These remarks will be made clearer in Sec. III.

This paper is organized as follows: In Sec. II we describe the four-coloring model on the square lattice, which is equivalent to the ground states of a particular Potts model. In Sec. III we map the four-coloring model onto an interface model and we introduce an ef-

fective field theory for the long-wavelength fluctuations of the interface. In Sec. IV we define different operators in the four-coloring model and we calculate their scaling dimensions; we find that they are given by the stiffness constant associated with the interface model. We turn our attention to the statistical and geometrical properties of loops that naturally appear in this model in Sec. V. In this section we also calculate the *exact* value of the stiffness, using recent results on the geometrical exponents of equal-height contour loops on random Gaussian surfaces.[19] Finally, in Sec. VI, we present our Monte Carlo results for the stiffness, the scaling dimensions of operators, and the geometrical exponents associated with loops of alternating color. We conclude with a discussion of the conformal field theory of the four-coloring model, finite temperature properties of the Potts model (for which the four-coloring model is the ground-state ensemble), and an interpretation of the four-coloring model as a type of a fully packed loop model on the square lattice.

II. THE FOUR-COLORING MODEL

In this section we introduce the four-coloring model as the ground-state ensemble of the antiferromagnetic four-state Potts *vertex* model on the square lattice.

Our starting point is the antiferromagnetic Potts vertex model given by the Hamiltonian

$$\mathcal{H} = J \sum_{\mathbf{r}} \sum_{\substack{i,j=1 \\ i<j}}^{4} \delta(\sigma_i(\mathbf{r}), \sigma_j(\mathbf{r})) \ , \tag{2.1}$$

where the Potts spins $\sigma_i(\mathbf{r})(i = 1,2,3,4)$ live on the bonds of the square lattice $\{\mathbf{r}\}$, as shown in Fig. 1, and each spin can be in one of four possible states labeled A, B, C, and D. This Hamiltonian associates an energy penalty to having equal spins on bonds that share a vertex of the square lattice. An alternative representation of this model, introduced by Read,[14] involves the "crossed-square" lattice in which diagonal bonds are drawn on every other square plaquette, so that the "crossed" plaquettes form a checkerboard pattern. In this representation the Potts spins live on the *vertices* of the crossed-square lattice and have nearest-neighbor antiferromagnetic interactions.

At zero temperature, the only allowed spin configurations are ones for which $\{\sigma_1(\mathbf{r}), \sigma_2(\mathbf{r}), \sigma_3(\mathbf{r}), \sigma_4(\mathbf{r})\} = \{A, B, C, D\}$ for every $\mathbf{r}$. With $\{\sigma_1(\mathbf{r}), \sigma_2(\mathbf{r}), \sigma_3(\mathbf{r}), \sigma_4(\mathbf{r})\}$ we denote the *set* of Potts spins on the four bonds at the vertex $\mathbf{r}$, while by the *ordered set* $(\sigma_1(\mathbf{r}), \sigma_2(\mathbf{r}), \sigma_3(\mathbf{r}), \sigma_4(\mathbf{r}))$ we denote the particular configuration of spins at $\mathbf{r}$.

The ground-state ensemble has an extensive entropy. Namely, the ground-state entropy per site, defined as[3]

$$s = \lim_{N \to \infty} \frac{1}{N} \ln(Z_0), \tag{2.2}$$

where Z_0 is the number of ground states and

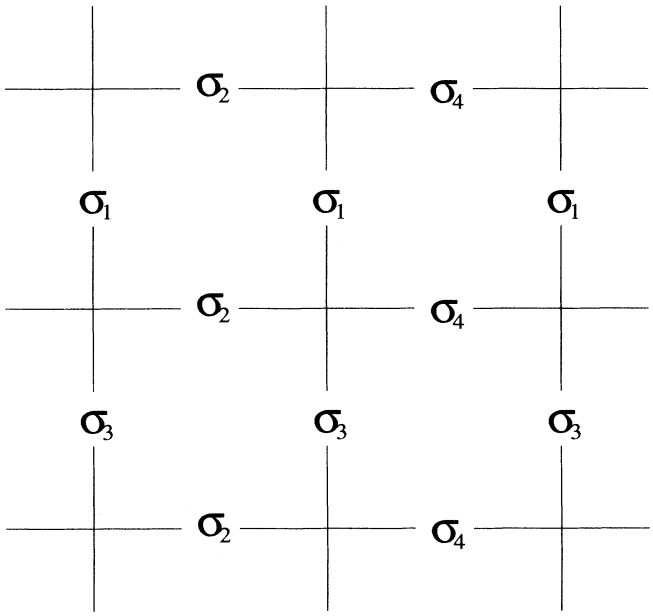

FIG. 1. Labeling of the spins in the Potts model. At each vertex of the square lattice $\mathbf{r}$, the four spins living on the bonds originating at $\mathbf{r}$ are labeled in a staggered manner.

N the number of sites, is nonzero. This can be easily verified by examining the state given in Fig. 2: In every AB plaquette the spins A and B can be exchanged independently of the other plaquettes. This gives rise to $2^{N/4}$ states, which puts a lower bound on the entropy per site at $s > \ln 2/4$.

If we think of the four Potts spins as four colors, then

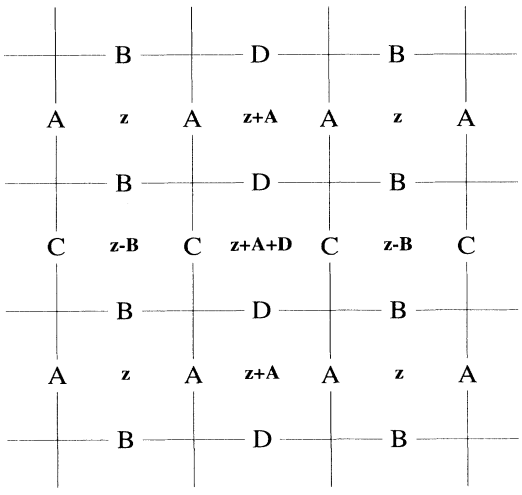

FIG. 2. One of 24 symmetry related ideal states of the four-coloring model. Using the height rule defined in the text, every plaquette is assigned a microscopic height $\mathbf{z}$. Note that in the ideal state the height describes, on average, a flat interface with a fast modulation of the microscopic height; the wavelength of the modulation is given by the lattice spacing. These fast modulations are responsible for the peak structure of the Fourier transformed microscopic height (see Fig. 6).

the ground states correspond to the four-coloring model on the square lattice. In the four-coloring model each bond of the square lattice is colored with one of four different colors A, B, C, or D, with the constraint that at each vertex all four colors meet. All such configurations are given the same statistical weight.

III. THE INTERFACE MODEL

In this section we describe the mapping of the four-coloring model to an interface model, and we propose an effective field theory that describes the long-wavelength fluctuations of this interface.

We define a height mapping by placing a three-component *microscopic height* $\mathbf{z} \in \mathbf{Z}^3$ at the center of each elementary square (plaquette) in such a way that the change in $\mathbf{z}$, when going from one plaquette to a neighboring one, is given by

$$\mathbf{z}\left(\mathbf{r}+\frac{\boldsymbol{\delta}}{2}\right)-\mathbf{z}\left(\mathbf{r}-\frac{\boldsymbol{\delta}}{2}\right)=(-1)^{(x+y)}\boldsymbol{\sigma}(\mathbf{r})\,, \tag{3.1}$$

where $\boldsymbol{\delta}$ crosses the bond that the color (spin) $\boldsymbol{\sigma}(\mathbf{r})$ lives on, and x and y are the components of $\mathbf{r}$. The phase factor on the right-hand side of the above equation accounts for the choice of direction in which the microscopic height increases (Fig. 2). The four possible color values that $\boldsymbol{\sigma}(\mathbf{r})$ can take are represented by vectors pointing to the vertices of a tetrahedron:

$$\begin{aligned}&\mathbf{A}=(-1,+1,+1), \quad \mathbf{B}=(+1,+1,-1),\\ &\mathbf{C}=(-1,-1,-1), \quad \mathbf{D}=(+1,-1,+1)\,.\end{aligned} \tag{3.2}$$

For a given configuration of colors, the set of microscopic heights defines a two-dimensional interface in five dimensions. Each allowed microscopic height configuration is given equal statistical weight.

In order to define an effective field theory for the above described interface model, we introduce a coarse-graining procedure for the microscopic heights in the following way (see Fig. 3 for a summary).

First, we define *ideal states* of the four-coloring model as states in which each plaquette is colored by two colors only (Fig. 2). There are $24 = 4!$ ideal states related to each other by lattice symmetries, and each corresponds to a different permutation of the four colors. These states are flat, in the sense that the variance of the microscopic height is minimum. Furthermore, they have the important property that most of the entropy of the four-coloring model is contained in bounded fluctuations around the ideal states. This point is crucial. Namely, if we wish to change the color of a bond, the smallest change we can perform on the lattice, without violating the constraints of the four-coloring model, is an exchange of two colors along a loop of alternating color. The ideal states *maximize* the number of loops of alternating color, and it is this property that selects them out. This entropic selection effect is similar in spirit to the "order by disorder" effect, introduced by Villain.[20]

Second, we replace the original model with a coarse-grained version where the lattice is split into domains, such that in each domain fluctuations occur about a different ideal state, as shown in Fig. 3. With each ideal-state domain we associate a *coarse-grained* height $\mathbf{h}$, which is given by the average microscopic height in that domain:

$$\mathbf{h}=\overline{\mathbf{z}}\,. \tag{3.3}$$

Third, we define the *ideal state graph* $\mathcal{I} \subset \mathbf{R}^3$. Every node of $\mathcal{I}$ represents an ideal state, and its position in $\mathbf{R}^3$ is given by the coarse-grained height $\mathbf{h} \in \mathbf{R}^3$ of the ideal state it represents.

Finally, we consider the long-wavelength limit of the interface model, where the heights defined over particular ideal-state domains are replaced with a continuously varying height field $\mathbf{h}(\mathbf{r}) \equiv (h_1(\mathbf{r}), h_2(\mathbf{r}), h_3(\mathbf{r}))$, as seen in Fig. 3. The dimensionless free energy f, of the interface, which is entropic in origin, is assumed to be of the form

$$f=\int d^2\mathbf{r}\,\left[\frac{K}{2}(|\nabla h_1|^2+|\nabla h_2|^2+|\nabla h_3|^2)+V(\mathbf{h})\right], \tag{3.4}$$

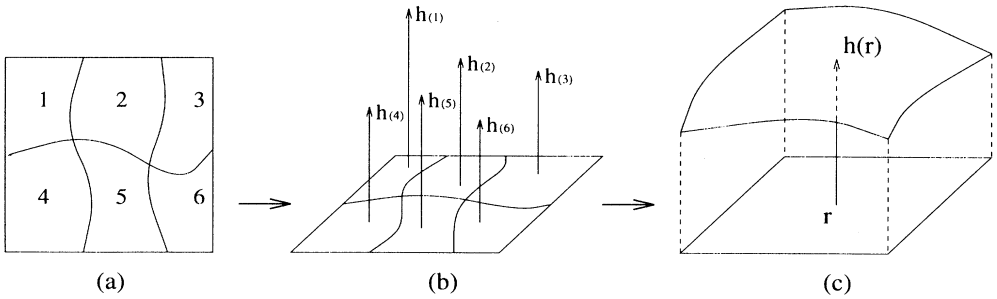

FIG. 3. The construction of a fluctuating interface equivalent to the four-coloring model (schematic): (a) The microscopic four-coloring state is broken up into domains of ideal states. The ideal states are here denoted by the integers $i = 1, 2, \ldots, 6$, and the set of microscopic heights for each ideal state is $\{\mathbf{z}\}_i$. (b) Each ideal-state domain is assigned a coarse-grained height equal to the average microscopic height of the domain, $\mathbf{h}_{(i)} = \overline{\{\mathbf{z}\}_i}$. (c) Finally, the discrete heights $\mathbf{h}_{(i)}$ are replaced by a continuous height field $\mathbf{h}(\mathbf{r})$; the interface is assumed to be rough. (This construction works for all known discrete spin models with critical ground states.[12])

where $V(\mathbf{h})$ is a periodic potential with the periodicity given by the ideal-state graph,

$$V(\mathbf{h}+\mathcal{I}) = V(\mathbf{h}) \,. \tag{3.5}$$

The free energy f defines an effective field theory of the four-coloring model; the assumption being made is that it correctly describes the long-wavelength fluctuations of the microscopic height $\mathbf{z}$. The periodic potential $V(\mathbf{h})$, which is usually referred to as the *locking term*,[21] favors the heights to take their values on $\mathcal{I}$, while the first term represents fluctuations around the flat ideal states. Therefore, the assumption that the effective field theory of the four-coloring model is given by Eq. (3.4) is directly related to the intuitive idea put forward earlier, that the free energy of the four-coloring model is entirely contained in bounded fluctuations around the ideal states.

The locking term is periodic with the periodicity of $\mathcal{I}$. Thus, the four-coloring model, in its interface representation, undergoes a roughening transition for some value of the stiffness $K = K_r$.[21] If the stiffness K satisfies $K < K_r$, then the locking term in Eq. (3.4) becomes irrelevant, in the renormalization group sense, and the four-coloring model is described by a Gaussian model with a free energy

$$f = \frac{K}{2} \int d^2\mathbf{r} \left(|\nabla h_1|^2 + |\nabla h_2|^2 + |\nabla h_3|^2 \right) . \tag{3.6}$$

In the case that the locking term is relevant ($K > K_r$), the four-coloring model will lock into long-range order in one of the ideal states. We will see later that in the interface representation of the four-coloring model K actually equals K_r, so the model is *at* the roughening transition.

IV. OPERATORS IN THE FOUR-COLORING MODEL

In this section we elaborate on the construction of the ideal-state graph, and we define operators in the four-coloring model that are periodic functions of the height. We show that the stiffness of the interface K determines the scaling dimensions of *all* the operators.

A. The ideal-state graph

The ideal-state graph $\mathcal{I}$, introduced in the preceding section, plays a crucial role in calculating the scaling dimensions of operators in the four-coloring model. Here we describe how we construct the ideal-state graph in more detail.

We start with an arbitrary ideal state; in order to be concrete let us take this state to be $(ABCD)$. If we exchange the colors A and B on all the AB plaquettes we get a new ideal state, $(BACD)$. Only the AB plaquettes are affected by these *loop updates*, and consequently only the microscopic heights defined at their centers are allowed to change. The change in $\mathbf{z}$ at the AB plaquettes is $\Delta\mathbf{z} = \mathbf{A} - \mathbf{B}$, which gives rise to a change of the coarse grained height of $\Delta\mathbf{h} = 1/4\ \Delta\mathbf{z} = 1/4\ (\mathbf{A}-\mathbf{B})$; this is the vector that takes us from the node $(ABCD)$ to the node $(BACD)$ on the graph $\mathcal{I}$. Note that in this way the edges of $\mathcal{I}$ are associated with transpositions of the colors. Repeating this procedure we construct the ideal-state graph which is shown in Fig. 4.

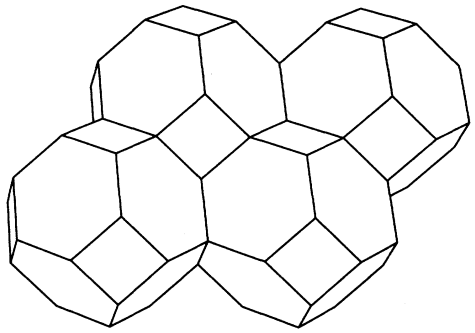

FIG. 4. The ideal-state graph of the four-coloring model. The vertices that correspond to the 24 different ideal states form a truncated octahedron. The full ideal-state graph corresponds to a periodic tiling of space with these octahedra. They are arranged in a face-centered-cubic lattice.

The 24 *different* ideal states form a truncated octahedron with a side of length $\sqrt{2}/2$ in the units chosen for the vectors $\mathbf{A}$, $\mathbf{B}$, $\mathbf{C}$ and $\mathbf{D}$; see Fig. 4. These truncated octahedra are arranged *periodically* in a face-centered-cubic (fcc) lattice, which we call the *direct lattice* $\mathcal{D}$, to form the full ideal-state graph. The side of the conventional cubic cell of $\mathcal{D}$ is 4.

B. Definitions of operators

In order to define local operators on the lattice as functions of the colors, we adopt the vector representation of the four colors Eq. (3.2). We define operators in such a way that they are spatially uniform in the ideal states.

A local operator $O(\mathbf{r})$ constructed from the colors and spatially uniform in the ideal states can be written in terms of the coarse-grained height as $\overline{O}(\mathbf{h}(\mathbf{r}))$. Since $\mathbf{h}$ and $\mathbf{h}+\mathcal{D}$ represent the same ideal state on the ideal-state graph, we can identify them

$$\mathbf{h} \equiv \mathbf{h} + \mathcal{D} \,, \tag{4.1}$$

and the operator $\overline{O}(\mathbf{h})$ is necessarily periodic with the periods forming the fcc lattice $\mathcal{D}$. Therefore, we can write $O(\mathbf{r})$ as a Fourier series

$$O(\mathbf{r}) = \sum_{\mathbf{G}\in\mathcal{R}} O_{\mathbf{G}} e^{i\mathbf{G}\cdot\mathbf{h}(\mathbf{r})} \,, \tag{4.2}$$

where $\mathcal{R}$ is the body-centered-cubic lattice (bcc) *reciprocal* to the direct lattice;[22] it has a conventional cubic cell of side π. The scaling dimension of $O(\mathbf{r})$ is equal to the scaling dimension of the most relevant operator in the above expansion.

We define four operators: the staggered spin, the row-staggered spin, the cross-staggered spin, and the par-

ity. All four are functions of the color configuration $(\boldsymbol{\sigma}_1(\mathbf{r}), \boldsymbol{\sigma}_2(\mathbf{r}), \boldsymbol{\sigma}_3(\mathbf{r}), \boldsymbol{\sigma}_4(\mathbf{r}))$ of the bonds that share the common vertex $\mathbf{r}$. More abstractly, every color configuration at a vertex is a permutation of the four colors, and these operators can be thought of as functions on the permutation group S_4.

The *staggered spin* $\mathbf{S}(\mathbf{r})$ is defined as

$$\mathbf{S}(\mathbf{r}) = \boldsymbol{\sigma}_1(\mathbf{r}) + i\boldsymbol{\sigma}_2(\mathbf{r}) - \boldsymbol{\sigma}_3(\mathbf{r}) - i\boldsymbol{\sigma}_4(\mathbf{r}) \,. \tag{4.3}$$

The staggered spin takes its values in the three-dimensional complex space $\mathbf{C}^3$. This operator returns different values for all the 24 ideal states (elements of the permutation group) and therefore plays the role of the order parameter in the four-coloring model. The reciprocal lattice vector of the most relevant term in Eq. (4.2) for the operator $\mathbf{S}(\mathbf{r})$ is

$$\mathbf{G}_S = \pi\left(\frac{1}{2}, \frac{1}{2}, \frac{1}{2}\right). \tag{4.4}$$

The *row-staggered spin* $\mathbf{R}(\mathbf{r})$ is defined as

$$\mathbf{R}(\mathbf{r}) = \boldsymbol{\sigma}_1(\mathbf{r}) - \boldsymbol{\sigma}_2(\mathbf{r}) + \boldsymbol{\sigma}_3(\mathbf{r}) - \boldsymbol{\sigma}_4(\mathbf{r}) \,. \tag{4.5}$$

This operator maps elements of the permutation group to vectors in $\mathbf{R}^3$. It returns equal values for ideal states related by a (13)(24) permutation [the notation (pq) means transpose p and q]. In the ideal-state graph, states related by a (13)(24) permutation are separated by $[2,0,0]$ type vectors, and therefore we conclude that the reciprocal lattice vector of the most relevant operator in the Fourier expansion of $\mathbf{R}(\mathbf{r})$ is

$$\mathbf{G}_R = \pi(1,0,0) \,. \tag{4.6}$$

The *parity* $\mathbf{P}(\mathbf{r})$ takes two different values depending on whether the color permutation $(\boldsymbol{\sigma}_1(\mathbf{r}), \boldsymbol{\sigma}_2(\mathbf{r}), \boldsymbol{\sigma}_3(\mathbf{r}), \boldsymbol{\sigma}_4(\mathbf{r}))$ is even or odd. It can be defined as the triple product

$$\mathbf{P}(\mathbf{r}) = \boldsymbol{\sigma}_1(\mathbf{r}) \cdot (\boldsymbol{\sigma}_2(\mathbf{r}) \times \boldsymbol{\sigma}_3(\mathbf{r})) \,. \tag{4.7}$$

Since each bond of the ideal-state graph corresponds to a single transposition of the colors, the parity changes sign when going from one ideal state to the neighboring one. It has the same periodicity as the row-staggered spin, and the associated reciprocal lattice vector is

$$\mathbf{G}_P = \pi(1,0,0) \,. \tag{4.8}$$

Finally, we define the *cross-staggered spin* as

$$\mathbf{Q}(\mathbf{r}) = [\boldsymbol{\sigma}_1(\mathbf{r}) - \boldsymbol{\sigma}_3(\mathbf{r})] \times [\boldsymbol{\sigma}_2(\mathbf{r}) - \boldsymbol{\sigma}_4(\mathbf{r})] \,. \tag{4.9}$$

The periods of $\mathbf{Q}(\mathbf{r})$ are vectors of the type $[2,0,0]$ and $[1,1,1]$ in the ideal-state graph (they generate a bcc lattice which is the Bravais lattice[22] of the ideal-state graph), and therefore its most relevant reciprocal lattice vector is

$$\mathbf{G}_Q = \pi(1,1,0) \,. \tag{4.10}$$

C. Scaling dimensions

Using Eq. (3.6) for the free energy, we can easily calculate the scaling dimensions of the staggered spin, the row-staggered spin, the parity, and the cross-staggered spin. They are given by the scaling dimension of the most relevant operator appearing in their respective Fourier expansions, Eq. (4.2).

The scaling dimension $x_{\mathbf{G}}$ of an operator of the form $\exp(i\mathbf{G}\cdot\mathbf{h}(\mathbf{r}))$ figures in the two-point correlation function

$$\langle e^{i\mathbf{G}\cdot\mathbf{h}(\mathbf{0})} e^{-i\mathbf{G}\cdot\mathbf{h}(\mathbf{r})} \rangle \sim \frac{1}{r^{2x_{\mathbf{G}}}} \,, \tag{4.11}$$

where the averaging is with respect to the Gaussian free energy Eq. (3.6); here we have assumed that the locking term in Eq. (3.4) is irrelevant. Using the property of the Gaussian model, that the average of the square of the height difference varies logarithmically with separation,

$$\langle (h_j(0) - h_i(\mathbf{r}))^2 \rangle = \delta_{ij} \frac{1}{\pi K} \ln(r) + \text{const} \,, \tag{4.12}$$

we find the scaling given by Eq. (4.11), where the scaling dimension is

$$x_{\mathbf{G}} = \frac{1}{2\pi K} \frac{|\mathbf{G}|^2}{2} \,. \tag{4.13}$$

It is important to note that the stiffness K completely determines the scaling dimensions of *all* the operators in the four-coloring model; $\mathbf{G}$ in Eq. (4.13) is the most relevant reciprocal lattice vector. This is a well-known scenario that appears in two-dimensional models that renormalize, at the critical point, to the vacuum phase of the Coulomb gas.[13]

The assumption that the locking term in Eq. (3.4) is irrelevant corresponds to the condition[13]

$$x_{\mathbf{G}_\mathcal{I}} \geq 2 \,, \tag{4.14}$$

where $\mathbf{G}_\mathcal{I} \in \mathcal{R}$ is the periodicity of the ideal-state graph, which is the periodicity of the potential $V(\mathbf{h})$. Looking at Fig. 4 we see that the Bravais lattice of the ideal-state graph is a bcc lattice with a conventional cubic cell whose side is of length 2; this implies $\mathbf{G}_\mathcal{I} = \pi(1,1,0)$. Now, using Eq. (4.13), we can rewrite the condition Eq. (4.14) as a condition on the inverse stiffness,

$$K^{-1} \geq \frac{4}{\pi} = 1.273\ldots \,. \tag{4.15}$$

We will see in the following section that the value of the stiffness satisfies the above inequality as an equality, and that the four-coloring model in the interface representation is exactly *at* the roughening transition.

V. LOOPS IN THE FOUR-COLORING MODEL

In this section we study geometrical exponents associated with loops of alternating color: the loop size distribution exponent $\tau - 1$, the fractal dimension D, and the loop correlation function exponent x_1. Using recent

results on the statistical topography of rough interfaces we calculate these exponents *exactly*, which also leads to the exact value of the stiffness.

A. Definitions and scaling relations

The loop size distribution $P(s)$ is defined as the probability, given we choose a pair of colors $\alpha\beta$, that a loop of alternating color $\alpha\beta\alpha\beta\ldots$ passing through a fixed point on the lattice has a length s. Assuming that the four-coloring model is critical we can expect loops of all sizes to be present on the lattice; the smallest loop will be determined by the lattice spacing, while the largest loop will be given by the system size. Consequently, $P(s)$ is given by a power law

$$P(s) \sim s^{-(\tau-1)} . \tag{5.1}$$

The fractal dimension D of the loops in the four-coloring model determines the scaling of the length of a loop s with its radius R:

$$s \sim R^D . \tag{5.2}$$

The radius of a loop is defined as the side of the smallest box that contains the loop.

The fractal dimension and the loop size distribution exponent have been shown to satisfy the following scaling relations:[19,23,24]

$$\begin{aligned} \tau - 1 &= \frac{2}{2 - x_1} \\ D &= 2 - x_1 , \end{aligned} \tag{5.3}$$

where x_1 is the exponent that governs the behavior of the loop correlation function $\mathcal{G}_1(\mathbf{R})$. The loop correlation function is defined as the probability that two points that are separated by $\mathbf{R}$ lie on the same loop of alternating color.

The exponent x_1 can be calculated from the interface representation of the four-coloring model in the familiar way:[13] If we denote the number of configurations with a loop of alternating color passing through points 0 and $\mathbf{R}$ as $Z(\mathbf{R})$, then $\mathcal{G}_1(\mathbf{R})$ can be written as

$$\mathcal{G}_1(\mathbf{R}) = \frac{Z(\mathbf{R})}{Z} , \tag{5.4}$$

where Z is the total number of configurations; Z is also the partition function, since all configurations in the four-coloring model have equal statistical weight. Now, if we exchange the two colors on the loop along one half of the loop going from 0 to $\mathbf{R}$, then this generates a vortex and an antivortex in the interface model, at these two points. For example, if the loop consists of alternating A and B colored bonds, then the color configuration, after flipping half the loop, is A, A, C, D at one end, and B, B, C, D at the other (see Fig. 5). Using the height rule we find that the Burgers vectors associated with these "defects" are

$$\mathbf{b}_1 = \pm(\mathbf{A} - \mathbf{B}) = \pm(-2, 0, 2) . \tag{5.5}$$

Therefore, the loop correlation function is equal to the probability of having a vortex-antivortex pair of Burgers charge $\mathbf{b}_1$ separated by $\mathbf{R}$, in the interface model. This probability is readily calculated using the formula for the free energy of the interface in terms of the coarse-grained height Eq. (3.6). It follows from Eq. (3.6) that the energy of a vortex pair varies logarithmically with separation R, and from this it can be shown that[13]

$$\mathcal{G}_1(\mathbf{R}) \sim |\mathbf{R}|^{-2x_1} , \tag{5.6}$$

where the exponent x_1 is determined by the stiffness

$$x_1 = \frac{K}{2\pi} \frac{|\mathbf{b}_1|^2}{2} . \tag{5.7}$$

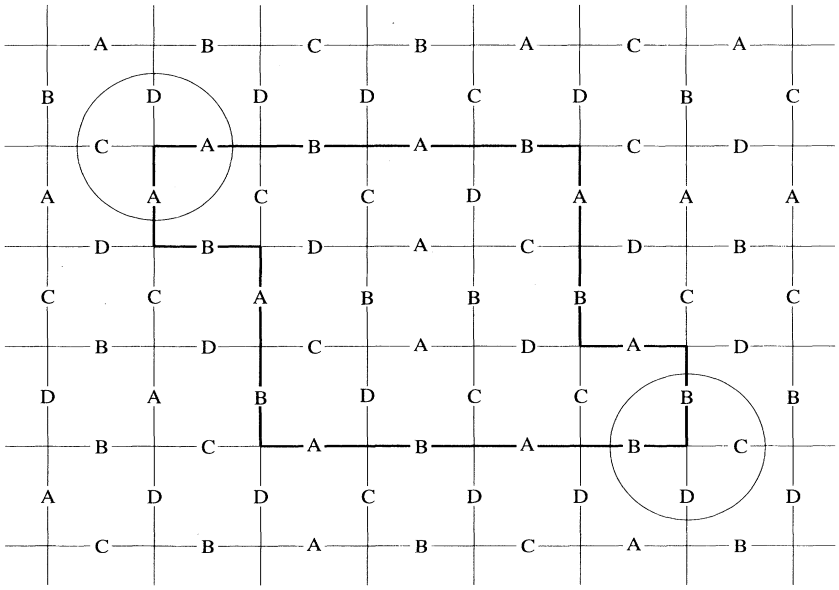

FIG. 5. A vortex-antivortex pair (circled) in the four-coloring model; the pair belongs to a loop of alternating color (bold). These defects are responsible for the behavior of the specific heat and the correlation length at small but finite temperatures.

B. Exact results from the statistical topography of Gaussian surfaces

In the interface representation, loops of alternating color become loops of constant height. This is most readily understood from an example: take an AB loop, and consider the points at the centers of the plaquettes along the inside of the loop (Fig. 5). These points are separated by C and D bonds only, and therefore the component of the microscopic height $\mathbf{z}$ in the $\mathbf{e}_1$-$\mathbf{e}_3$ direction is unchanged as we go around the loop (the projections of both $\mathbf{C}$ and $\mathbf{D}$ are zero in this direction; $\mathbf{e}_i$ are the orthonormal basis vectors in the height space). In general, every pair of colors defines loops of alternating color on the lattice, and they are contour lines of the component of $\mathbf{z}$ in the direction which is perpendicular to the vectors representing the other two colors.

This observation allows us to calculate *exactly* the loop correlation function $\mathcal{G}_1(\mathbf{R})$, by using the following result, that we have discussed elsewhere:[19] the probability that two points that are separated by $\mathbf{R}$ belong to the same equal height contour of a random Gaussian surface defined by Eq. (3.6) is universal, in other words, *independent* of the value of the stiffness, and given by

$$\mathcal{G}_1(\mathbf{R}) \sim |\mathbf{R}|^{-1} , \tag{5.8}$$

from which the exact result $x_1 = \frac{1}{2}$ follows. Inserting the latter value into Eq. (5.7) gives the exact value of the stiffness:

$$K^{-1} = \frac{4}{\pi} = 1.273\ldots . \tag{5.9}$$

As advertised earlier, the exact value of K satisfies Eq. (4.15) as an equality, and we conclude that the interface model is *at* the roughening transition. The exact scaling dimensions of operators in the four-coloring model are completely determined by K; their values are given in Table I.

From the scaling relations Eq. (5.3) and using the exact value of the defect exponent $x_1 = \frac{1}{2}$, we can also calculate the exponent $\tau - 1$ and the fractal dimension D,

$$\begin{aligned} \tau - 1 &= \tfrac{4}{3} \\ D &= \tfrac{3}{2} . \end{aligned} \tag{5.10}$$

It is interesting to note that in the three-coloring model on the honeycomb lattice, which is defined as an equal-weighted edge coloring of the honeycomb lattice with three different colors, loops of alternating color also represent loops of constant height (in this model the height is a two-component vector).[5,8] In fact, for this model, the exponent $\tau - 1$ has been measured in numerical simulations by Chandra, Coleman, and Richey,[6] and they report $\tau - 1 = 1.34 \pm 0.02$, in excellent agreement with the exact result $\tau - 1 = 4/3$.

TABLE I. The scaling dimensions of the operators in the four-coloring model; $x_O^{(1)}$ was calculated from the value of the stiffness found numerically, $K^{-1} = 1.28 \pm 0.01$ (Sec. VI), $x_O^{(2)}$ was determined from the structure factor of the staggered spin and the row-staggered spin (Sec. VI), and x_O^{exact} was calculated using the exact value of the stiffness found from the statistical topography analysis of contour loops (Sec. V).

$O(\mathbf{r})$	$\mathbf{G}_O$	$x_O^{(1)}$	$x_O^{(2)}$	x_O^{exact}
$\mathbf{S}(\mathbf{r})$	$\pi(\frac{1}{2},\frac{1}{2},\frac{1}{2})$	0.754 ± 0.006	0.70 ± 0.03	$\frac{3}{4}$
$\mathbf{R}(\mathbf{r})$	$\pi(1,0,0)$	1.005 ± 0.008	0.96 ± 0.1	1
$\mathbf{P}(\mathbf{r})$	$\pi(1,0,0)$	1.005 ± 0.008		1
$\mathbf{Q}(\mathbf{r})$	$\pi(1,1,0)$	2.011 ± 0.016		2

VI. RESULTS FROM MONTE CARLO SIMULATIONS

In this section we present our Monte Carlo results for the stiffness, the staggered spin and row-staggered spin structure factors (from which the scaling dimensions of these two operators can be deduced), and the fractal dimension and size distribution of loops of alternating color.

A. The stiffness

In order to determine the stiffness and check that the interface model is indeed rough, we have performed Monte Carlo simulations of the four-coloring model on square lattices of size 16×16, 32×32, and 64×64. Periodic boundary conditions were imposed and the system was equilibrated by performing loop updates, which, as pointed out earlier, are the smallest possible changes on the lattice that leave all the constraints of the four-coloring model satisfied.

A loop update consists of choosing a bond and one of its nearest neighbors at random; these two bonds will necessarily be of different color, say A and B. Next we follow the AB loop to which the two chosen bonds belong; due to the periodic boundary conditions the loop actually lives on a torus. If the loop has winding numbers in both directions equal to zero, we exchange colors A and B over the length of the whole loop. This will result in a new ground state. (We update only the loops with zero winding numbers to ensure that the overall tilt of the interface is kept at zero.)

In order to satisfy detailed balance every proposed loop update is accepted, since all the microstates have equal statistical weight. The loop updates are ergodic in the sense that they can be used to go from one ideal state to all the others with the same overall tilt. (In the worst case some isolated states might not be attainable but they will not be macroscopically represented in the ground-state ensemble.)

At this point it is interesting to point out that a Monte Carlo simulation of the Potts model Eq. (2.1), at small but nonzero temperature T, should incorporate some sort of a cluster algorithm which approaches this loop algorithm in the $T \to 0$ limit; a single-spin-flip type of algorithm would fail completely in this limit. Monte Carlo simulations with loop updates have been recently studied as algorithms that reduce critical slowing down by Evertz, Lana, and Marcu.[25]

The initial configuration was chosen to be either flat (i.e., an ideal state) or corresponding to a "roof" configuration in which the interface rises uniformly, starting from two opposite sides of the lattice. For the "roof" configuration on the 64×64 lattice we found that approximately 600 loop updates were needed to flatten the "roof"; in other words, the equilibration time at this system size is roughly 600 loop updates. Measurements of the microscopic height were performed only at intervals of an equilibration time in order to avoid measuring the height over states that were very correlated. We did not obtain a more quantitative measure of the dynamics of the four-coloring model with loop updates, which can be done by measuring the equilibration time as a function of the system size.[25] We believe this to be an interesting open problem.

After the system is equilibrated we construct the microscopic heights $\{\mathbf{z}(\mathbf{r})\}$ using the height rule Eq. (3.1). From this we calculate, using a fast Fourier transform routine,[26] the Fourier transformed microscopic heights $\{\tilde{\mathbf{z}}(\mathbf{q})\}$. This is repeated for many equilibrated states and we calculate the average value of the modulus squared of each Fourier component $\{\langle|\tilde{z}_i(\mathbf{q})|^2\rangle, (i = 1, 2, 3)\}$ and its variance.

Assuming that the long-wavelength fluctuations of the microscopic height are correctly described by the Gaussian free energy Eq. (3.6), we expect from equipartition:

$$\lim_{\mathbf{q}\to 0} \mathbf{q}^2 \langle|\tilde{z}_i(\mathbf{q})|^2\rangle = K^{-1}, \ (i = 1, 2, 3) \ . \tag{6.1}$$

The results from the simulation are plotted in Fig. 6 where we show data for the first height component; the plots for the other two components are identical (within error bars), as expected from symmetry. The data shown are for a 64×64 lattice; no appreciable finite size effects were found when results from different system sizes were compared. The construction of the microscopic heights was performed every 600 elementary loop updates, and a total of 6×10^4 measurements of the Fourier transformed microscopic height were taken (this took a few days on a Sun-Sparc1 station). These were grouped in 100 bunches of 600 successive measurements. The average values of $|\tilde{z}_1(\mathbf{q})|^2$ over each bunch were considered independent, and the error bars seen in Fig. 6 were obtained from their variance over the 100 bunches.

From the plot we see that the Fourier transformed heights indeed behave as required by Eq. (6.1), and we conclude that the interface is rough. From the intercept of the plot, we determine the inverse stiffness to be

$$K^{-1} = 1.280 \pm 0.010 \ . \tag{6.2}$$

This is in excellent agreement with the exact value of the stiffness given in Eq. (5.9). The above value of the stiffness was determined by fitting $\langle|\tilde{z}_1(\mathbf{q})|^2\rangle$ to the function $\mathbf{q}^{-2}(K^{-1} + C_1\mathbf{q}^2 + C_2 q_x^2 q_y^2)$, which has the required symmetry of the lattice, and it minimizes the standard deviation. Data for wave vectors within the outermost squarelike contour on the contour plot shown in Fig. 7 were used for the fit. The parameters C_1 and C_2 were found to be 0.355 ± 0.003 and -0.44 ± 0.02, respectively.

Prominent features in the plot in Fig. 6 are the peak at $\mathbf{q}^2 = \pi^2 = 9.869\ldots$ and the smaller peak at $\mathbf{q}^2 =$

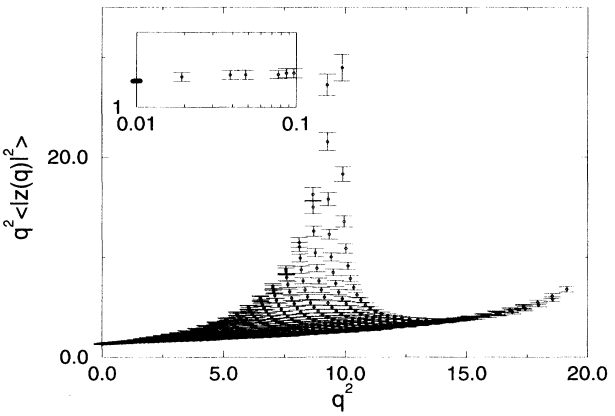

FIG. 6. The Monte Carlo data for the Fourier transformed microscopic height. What are shown are data for the first height component; the other two are equivalent, within error bars. The size of the system for which we show the data was 64×64, and the wave vector $\mathbf{q}$ was measured in units of the inverse lattice spacing. Note that in the limit $\mathbf{q} \to 0$, $\mathbf{q}^2\langle|\tilde{z}(\mathbf{q})|^2\rangle$ approaches a finite nonzero value, as expected for a rough interface. The peaks at $\mathbf{q}^2 = \pi^2 = 9.869\ldots$ and $\mathbf{q}^2 = 2\pi^2 = 19.739\ldots$ are a consequence of the modulation of the microscopic height in the ideal states. In the inset we show the same data on a log-log plot, at the smallest values of $\mathbf{q}$. The mark on the vertical axis corresponds to the exact value of the stiffness $K^{-1} = 4/\pi = 1.273\ldots$, found in Sec. V.

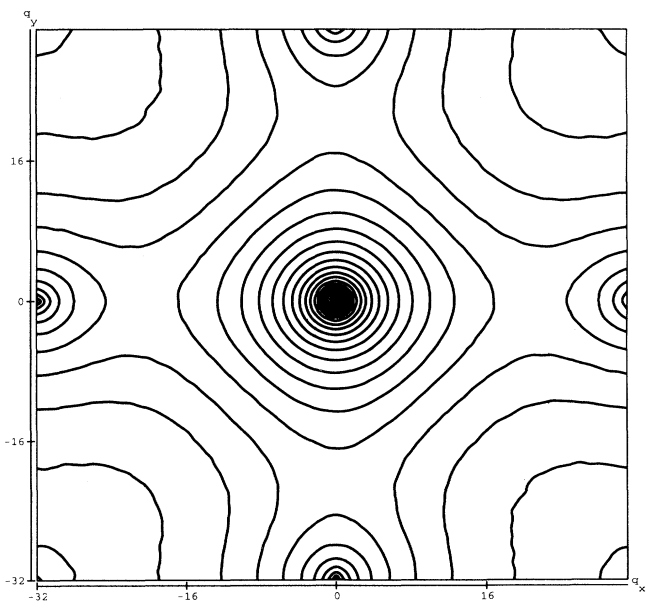

FIG. 7. The contour plot of $\ln(\langle|\tilde{z}(\mathbf{q})|^2\rangle)$ for system size 64×64; $\mathbf{q}$ is in units $2\pi/64$. Note the peaks at $\mathbf{q} = (32, 0)$, $(0, 32)$, and $(32, 32)$ (and at the symmetry related points); data within the outermost squarelike contour, centered around $(0, 0)$, were used in extracting the value of the stiffness.

$2\pi^2 = 19.739\ldots$. They appear due to the fact that the microscopic height is not uniform in an ideal state but is rapidly oscillating with wave vectors $\mathbf{Q} = (\pi, 0)$, $(0, \pi)$, and (π, π). This results in $\tilde{z}_1(\mathbf{q})$ having delta-function peaks at $\mathbf{q} = \mathbf{Q}$ in an ideal state, which are smeared out by fluctuations around the ideal state. Actually, these peaks carry information about the staggered spin and row-staggered spin structure factors, which we discuss next.

B. Structure factors of operators

Due to the linear connection between the microscopic heights and the spins Eq. (3.1), we can express the structure factor of the staggered spin and row-staggered spin in terms of the height structure factor $\tilde{\mathbf{z}}(\mathbf{q})$.

If we substitute Eq. (3.1) into the defining equation for the staggered spin Eq. (4.3), then, after Fourier transforming, we find that the structure factor of this operator is given by

$$|\widetilde{\mathrm{Re}S_i}(\mathbf{q}+(\pi,0))|^2 = 16|\tilde{z}_i(\mathbf{q})|^2 \times \sin^2\left(\frac{q_x}{2}\right)\cos^2\left(\frac{q_y}{2}\right), \quad (6.3)$$

where $\mathrm{Re}S_i$ is the real part of the ith component of the staggered spin. The formula for the imaginary part has q_x and q_y interchanged, and instead of the shift $(\pi, 0)$ we have a shift of $(0, \pi)$.

Similarly, from Eq. (3.1) and Eq. (4.5) we find that the structure factors for the row-staggered spin and the microscopic height are related by

$$|\widetilde{R_i}(\mathbf{q}+(\pi,\pi))|^2 = 64|\tilde{z}_i(\mathbf{q})|^2 \times \sin^2\left(\frac{q_x}{2}\right)\sin^2\left(\frac{q_y}{2}\right). \quad (6.4)$$

In Fig. 8 we show the plots for $\langle|\widetilde{\mathrm{Re}S_1}(\mathbf{q}|^2\rangle$ and $\langle|\widetilde{R_1}(\mathbf{q}|^2\rangle$, which were computed from Eqs. (6.3) and (6.4), using the data for $\langle|\tilde{z}_1(\mathbf{q})|^2\rangle$ shown in Fig. 6. We see from the plots that at small wave vectors both structure factors decay approximately as power laws. This explains the peaks seen in the plot of the height structure factor at $\mathbf{q} = (\pi, 0)$, $(0, \pi)$, and (π, π) (Fig. 7).

The power law decay of the structure factor is to be expected for operators that have autocorrelation functions that decay with distance as power laws:

$$\langle O(\mathbf{r})O(0)\rangle \sim \frac{1}{r^{2x_O}}. \quad (6.5)$$

Namely, if we Fourier transform the above equation, we find that for small wave vectors, the structure factor is given by

$$\langle|\tilde{O}(\mathbf{q})|^2\rangle \sim \mathbf{q}^{2(x_O-1)}. \quad (6.6)$$

This allows us to estimate the scaling dimension x_O of an operator from the power law behavior of its structure factor at small wave vectors.

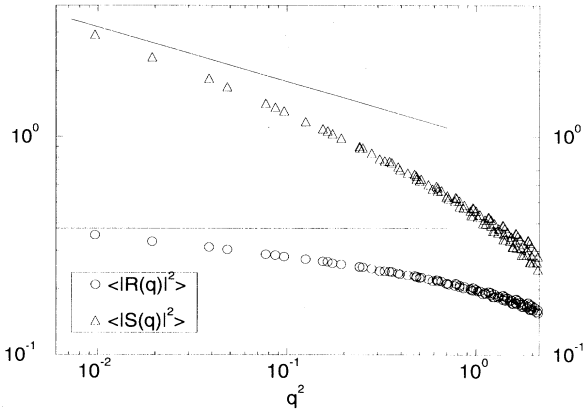

FIG. 8. The staggered spin $\langle|S(\mathbf{q})|^2\rangle$ and the row-staggered spin $\langle|R(\mathbf{q})|^2\rangle$ structure factor for system size 64×64. Here we show data at small wave vectors; note the power law decay which signals a critical (power law) autocorrelation function. The straight lines correspond to exact values of the scaling dimensions for these two operators ($x_S = \frac{3}{4}$ and $x_R = 1$) found in Secs. IV and V.

Fitting the data in Fig. 8 to a power law where $\langle|\tilde{O}(\mathbf{q})|^2\rangle = q^{2(x_O-1)}(C_1 + C_2 q)$ was chosen for the fitting function, with x_0, C_1, and C_2 being the fit parameters, gives for the scaling dimensions of the staggered spin and row-staggered spin

$$x_{\mathbf{S}}^{(2)} = 0.70 \pm 0.03 \quad (6.7)$$
$$x_{\mathbf{R}}^{(2)} = 0.96 \pm 0.01.$$

These are in good agreement with the exact values shown in Table I and the ones calculated from the value of the stiffness determined from simulations. They are both somewhat smaller than the exact values, which is most likely due to a relatively small system size (64×64).

It is important to note that the errors in Eq. (6.7) are about an order of magnitude worse than the errors for $x_{\mathbf{S}}^{(1)}$ and $x_{\mathbf{R}}^{(1)}$ in Table I, which were inferred *from the same data* by the method of calculating the exponents from the stiffness K which is extracted from $\langle|\tilde{z}_1(\mathbf{q})|^2\rangle$. We believe this demonstrates the superiority of the interface representation in extracting critical exponents from numerical data. Errors smaller by an order of magnitude were also found when the critical exponents for the antiferromagnetic Ising model of general spin on the triangular lattice, calculated using a height representation,[10] were compared to the values found using the more traditional finite size scaling method.[9]

C. The loop exponents

The exponents $\tau - 1$ and D defined in Eqs. (5.1) and (5.2) can be determined from Monte Carlo simulations. We record the length and radius of every loop that is updated. This allows us to plot the loop size distribution $P(s)$ and the mean length of a loop s as a function

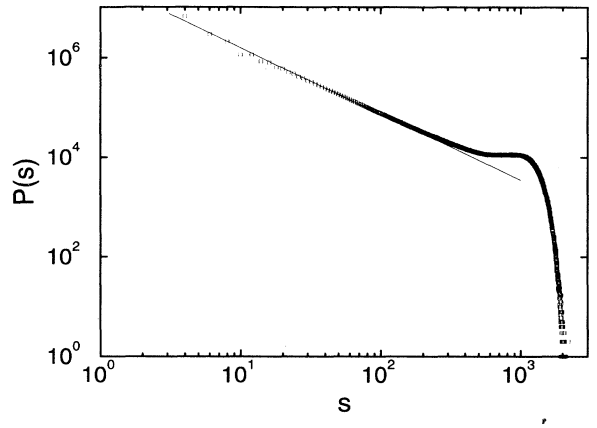

FIG. 9. The length distribution $P(s)$ of loops of alternating color in the four-coloring model. The distribution is cut off due to the finite system size (64×64). The line corresponds to a least squares fit to the data in the scaling region, $10 < s < 50$.

of the loop radius R (the radius was defined earlier as the side of the smallest square that completely covers the loop).

The results for system size 64×64 are shown in Figs. 9 and 10. We extract the value of $\tau - 1$ and D from the data in the scaling region by doing a least squares fit to a line, and we find

$$\tau - 1 = 1.30 \pm 0.03 \qquad (6.8)$$
$$D = 1.501 \pm 0.003 \, .$$

These numerical results are in excellent agreement with our analytic results displayed in Eq. (5.10), which relied on the interface representation of the four-coloring model. The measurements of $\tau - 1$ and D can also be thought

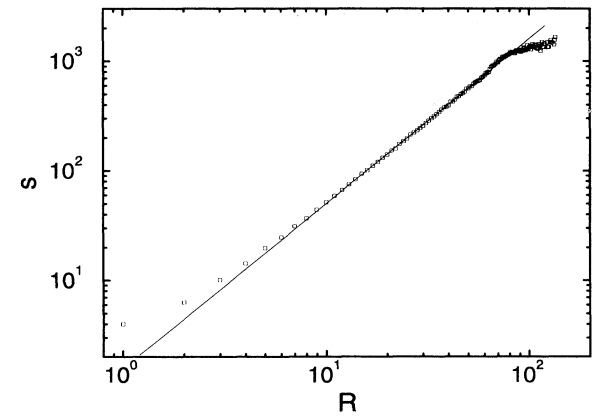

FIG. 10. The average length s of the loops in the four-coloring model as a function of their radius R. At small radii the length of a loop is constrained by the lattice spacing, while for very large loops the sytem size (64×64) intervenes. The line corresponds to a least squares fit to the data in the scaling region, $10 < R < 50$.

of as independent measurements of x_1 or of the stiffness K.

VII. DISCUSSION

We discuss the conformal field theory associated with the four-coloring model, finite temperature properties of the Potts vertex model, and the relation of the four-coloring model to a loop model.

A. Relation to conformal field theory

We have seen that the four-coloring model can be mapped onto a Gaussian interface Eq. (3.6) with a three-component height that is *compactified* on the direct lattice $\mathcal{D}$, Eq. (4.1). Thus, the CFT that emerges in the scaling limit is a rather simple one. It corresponds to three massless free bosons $\mathbf{h} = (h_1, h_2, h_3)$ [Eq. (3.6)], compactified on the fcc lattice. The fcc lattice is the root lattice of an SU(4) Lie algebra.[27] If the radius of compactification is carefully chosen, then the CFT has an additional infinite symmetry (besides the usual conformal symmetry described by the Virasoro algebra) given by the affine $SU(4)_{k=1}$ Kac-Moody algebra.[28] The choice of the radius of compactification is equivalent to the choice of the stiffness for the interface.

The idea that the scaling limit of the four-coloring model is given by the $SU(4)_{k=1}$ WZW model[15] was first put forward by Read.[14] He showed that the four-coloring model is equivalent to a lattice model with explicit SU(4) symmetry and went on to conjecture that the scaling limit is given by a WZW model. Our interface representation of the four-coloring model is thus a familiar construct in CFT; it corresponds to the free field representation of the $SU(4)_{k=1}$ WZW model.[29,30]

The conformal charge of the $SU(4)_{k=1}$ WZW model is $c = 3$, corresponding to the three free massless Bose fields (h_1, h_2, h_3). The operator spectrum of this CFT consists of three primary fields $\Phi(\mathbf{\Lambda}_i)$, $(i = 1, 2, 3)$ that transform under different representations of SU(4); by $\mathbf{\Lambda}_i$ we denote the highest weight of a representation of SU(4). The highest weights belong to the so-called weight lattice which is reciprocal to $\mathcal{D}$ and can therefore be identified with $\mathcal{R}$. In the free field representation, the primary fields of the CFT become exponentials of the Bose fields

$$\Phi(\mathbf{\Lambda}_i) = \exp\left(i\mathbf{\Lambda}_i \cdot \mathbf{h}(\mathbf{r})\right) , \qquad (7.1)$$

which are the so-called *vertex operators*. Their scaling dimensions are 3/4 (doubly degenerate) and 1,[27] which is in excellent agreement with our results shown in Table I. In fact, the exact values of the scaling dimensions shown in Table I, that were derived from the statistical topography of Gaussian surfaces, *prove* that the four-coloring model is in the universality class of the $SU(4)_{k=1}$ Wess-Zumino-Witten model. In other words, the fact that the three Bose fields are compactified on the fcc lattice, which is the root lattice of the SU(4) algebra,[27] and that K has the special value given by Eq. (5.9), proves the conjecture put forward by Read.

B. Predictions for finite temperature

At small but nonzero temperature, violations of the coloring rule (defects) are present in the Potts vertex model, which was defined in Eq. (2.1). The free energy is dominated by the elementary defects that cost the least amount of energy. These elementary defects in the Potts model have energy J and they come in pairs as seen in Fig. 5. In the interface representation they correspond to a vortex-antivortex pair with Burgers charge $\mathbf{b}_1$, Eq. (5.5).

The free energy f scales with the defect fugacity $Y_1 = \exp(-J/k_BT)$ as[13]

$$f \sim Y_1^{\frac{2}{2-x_1}} = Y_1^{\frac{4}{3}} , \tag{7.2}$$

where $x_1 = \frac{1}{2}$ is the previously determined vortex-antivortex correlation function exponent Eq. (5.8). This exponent also governs the scaling of the correlation length ξ with Y_1. Namely, the singular part of the free energy of the Potts vertex model is related to the correlation length by the hyperscaling relation

$$f \sim \xi^{-2} . \tag{7.3}$$

From Eq. (7.2) we find that the correlation length diverges with the defect fugacity (which goes to zero as the temperature approaches zero) as

$$\xi \sim Y_1^{-\frac{2}{3}} . \tag{7.4}$$

The scaling in Eq. (7.2) can in principle be checked by measuring the dependence of the specific heat on the fugacity, from Monte Carlo simulations of the Potts model at finite temperatures. This was done in the case of the three-state antiferromagnetic Potts model on the Kagomé lattice by Broholm *et al.*;[31] the ground states of this model correspond to the three-coloring model on the honeycomb lattice, which has been shown to be equivalent to a two-dimensional rough interface in *four* dimensions.[5] Elementary defects in this model also appear as vortex-antivortex pairs with the exponent $x_1 = \frac{1}{2}$.[8] Broholm *et al.* found the scaling given by Eq. (7.2) to hold, and they measured the exponent to be 1.3 ± 0.1, in good agreement with the exact result 4/3.

C. Relation to loop models

Recently there has been quite some interest in loop models on two-dimensional lattices.[7,32] The four-coloring model can be mapped to a fully packed double loop (FPDL) model on the square lattice. The FPDL model is defined by placing loops on the square lattice of two different flavors in such a way that each vertex belongs to two loops of different flavor, and every bond belongs to a single loop. We assign fugacities n_1 and n_2 to the two flavors of loops. Then the partition function of the FPDL model is given by

$$Z_0 = \sum_{\text{FP}} n_1^{N_1} n_2^{N_2} , \tag{7.5}$$

where the sum goes over all fully packed (FP) configurations, and N_1, N_2 are the number of loops of the first and second flavor, respectively. In the case $n_1 = n_2 = 2$ we recover the four-coloring model, where the two flavors of loops correspond to the AB and CD loops and the fugacities are due to the two possible ways of coloring each loop with alternating colors A-B and C-D.

An interesting line of inquiry, that we are currently pursuing, might be to understand the critical properties of the FPDL model for loop fugacities that are less than two. For higher loop fugacities we expect the associated interface model to be in the smooth phase. The loop model develops a finite correlation length that roughly corresponds to the radius of the largest loop in the system.

It is interesting to note that the $n_1 = n_2 = 1$ case is equivalent to the equal-weighted six-vertex model on the square lattice for which exact results are known.[3] The equal-weighted six-vertex model can be mapped to the three-state antiferromagnetic Potts model on the square lattice, which was found to possess a "mysterious" Z_4 symmetry.[33] We believe this Z_4 symmetry to be related to the SU(4) symmetry present in the four-coloring model. We are currently looking into this possibility.

The $n_1 = 2$, $n_2 = 1$ case is related to the dimer-loop model,[11] while the limit of vanishing fugacities might be an interesting new variant of the self-avoiding random walk problem.

VIII. CONCLUSION

We have investigated the critical properties of the four-coloring model. Making use of a mapping onto an interface model we have determined the scaling dimensions of different operators numerically, from a Monte Carlo simulation. We found that the numerical results are in excellent agreement with the values predicted from conformal field theory, which supports Read's conjecture[14] that the scaling limit of the four-coloring model is the $\text{SU}(4)_{k=1}$ Wess-Zumino-Witten model. We have also investigated numerically properties of loops of alternating color in the four-coloring model, and found excellent agreement with recent exact results on the geometry of equal-height contours on random Gaussian surfaces.[19] Finally, we demonstrated that the exact value of the stiffness $K = \pi/4$, which we extract from loop correlations in the Gaussian model, is sufficient to prove that the four-coloring model is in the universality class of the $\text{SU}(4)_{k=1}$ Wess-Zumino-Witten model.

We have not looked into the dynamics of the four-coloring model, which we believe to be worth investigating in view of the recent work on Monte Carlo algorithms with loop updates.[24] Further interesting questions

that we have only touched upon here are the finite temperature properties of the four-state antiferromagnetic Potts vertex model, and the critical properties of the fully packed double loop model away from the four-coloring point.

ACKNOWLEDGMENTS

We would like to thank A. LeClair for useful discussions. This work was supported by NSF Grant No. DMR-9214943.

[1] H. W. J. Blöte and H. J. Hilhorst, J. Phys. A **15**, L631 (1982).
[2] H. W. J. Blöte and M. P. Nightingale, Phys. Rev. B **47**, 15 046 (1993).
[3] E. H. Lieb and F. Y. Wu, in *Phase Transitions and Critical Phenomena*, edited by C. Domb and M. S. Green (Academic, London, 1972), Vol. 1.
[4] J.-S. Wang, R. H. Swendsen, and R. Kotecky, *ibid.* **63**, 109 (1989); H. Park and M. Widom, *ibid.* **63**, 1193 (1989).
[5] D. A. Huse and A. D. Rutenberg, Phys. Rev. B **45**, 7536 (1992).
[6] P. Chandra, P. Coleman, and I. Ritchey, J. Phys. I (France) **3**, 591 (1993).
[7] H. W. J. Blöte and B. Nienhuis, Phys. Rev. Lett. **72**, 1372 (1994).
[8] J. Kondev and C. L. Henley, Phys. Rev. Lett. **73**, 2786 (1994).
[9] O. Nagai, S. Miyashita, and T. Horiguchi, Phys. Rev. B **47**, 202 (1993).
[10] C. Zeng and C. L. Henley (unpublished).
[11] R. Raghavan, S. L. Arouh, and C. L. Henley (unpublished).
[12] C. L. Henley (unpublished).
[13] B. Nienhuis, in *Phase Transitions and Critical Phenomena*, edited by C. Domb and J. L. Lebowitz (Academic, London, 1987), Vol. 11.
[14] N. Read (unpublished).
[15] E. Witten, Commun. Math. Phys. **92**, 455 (1984).
[16] V. G. Knizhnik and A. B. Zamolodchikov, Nucl. Phys. **B247**, 83 (1984).
[17] J. M. Thijssen and H. J. F. Knops, Phys. Rev. B **42**, 2438 (1990).
[18] P. Ginsparg, in *Fields, Strings, and Critical Phenomena*, edited by E. Brézin and J. Zinn-Justin (North-Holland, Amsterdam, 1989).
[19] J. Kondev and C. L. Henley, Phys. Rev. Lett. **74**, 4580 (1995).
[20] J. Villain, R. Bidaux, J.-P. Carton, and R. Conte, J. Phys. (Paris) **41**, 1263 (1980).
[21] G. Forgacs, R. Lipowsky, and Th. M. Nieuwenhuizen, in *Phase Transitions and Critical Phenomena*, edited by C. Domb and J. L. Lebowitz (Academic, London, 1991), Vol. 14.
[22] N. W. Ashcroft and N. D. Mermin, *Solid State Physics* (Saunders, Philadelphia, 1976).
[23] H. Saleur and B. Duplantier, Phys. Rev. Lett. **58**, 2325 (1987).
[24] J. Cardy, in *Fluctuating Geometries in Statistical Mechanics and Field Theory*, edited by F. David, P. Ginsparg, and J. Zinn-Justin (Elsevier Science Publishers, New York, 1995).
[25] H. G. Evertz, G. Lana, and M. Marcu, Phys. Rev. Lett. **70**, 875 (1993).
[26] W. H. Press, B. P. Flannery, S. A. Teukolsky, and W. T. Vetterling, *Numerical Recipes in Fortran* (Cambridge University Press, Cambridge, 1988).
[27] J. Fuchs, *Affine Lie Algebras and Quantum Groups* (Cambridge University Press, Cambridge, 1992).
[28] J. Kondev and C. L. Henley (unpublished).
[29] I. B. Frenkel and V. G. Kac, Invent. Math. **62**, 23 (1980).
[30] G. Segal, Commun. Math. Phys. **80**, 301 (1981).
[31] C. Broholm, G. Aeppli, G. P. Espinoza, and A. S. Cooper, J. Appl. Phys. **69**, 4968 (1991).
[32] S. O. Waarnar, B. Nienhuis, and K. A. Seaton, Phys. Rev. Lett. **69**, 710 (1992).
[33] H. Saleur, Nucl. Phys. **B360**, 219 (1991).